Supporting Information

Novel bright blue emissions IIB group complexes constructed with various polyhedron-induced 2-[2′-(6-methoxy-pyridyl)]-benzimidazole derivatives

Shuo Chen, Rui-Qing Fan,* Xin-Ming Wang and Yu-Lin Yang*

* Department of Chemistry, Harbin Institute of Technology, Harbin 150001, P. R. of China

Index

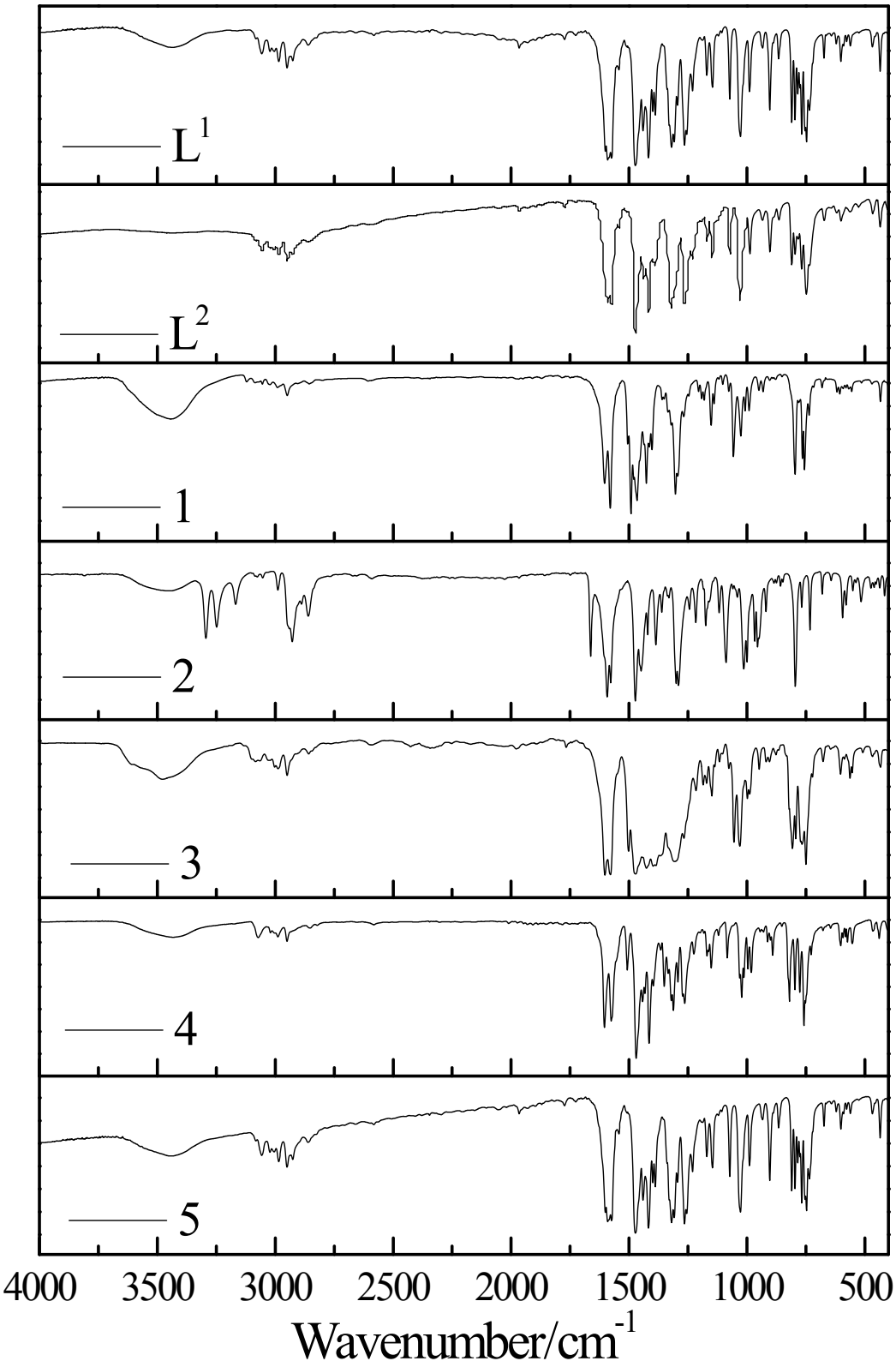

Figure S1. Infrared spectra of **L** and complexes **1**–**5** recorded from a KBr pellet.

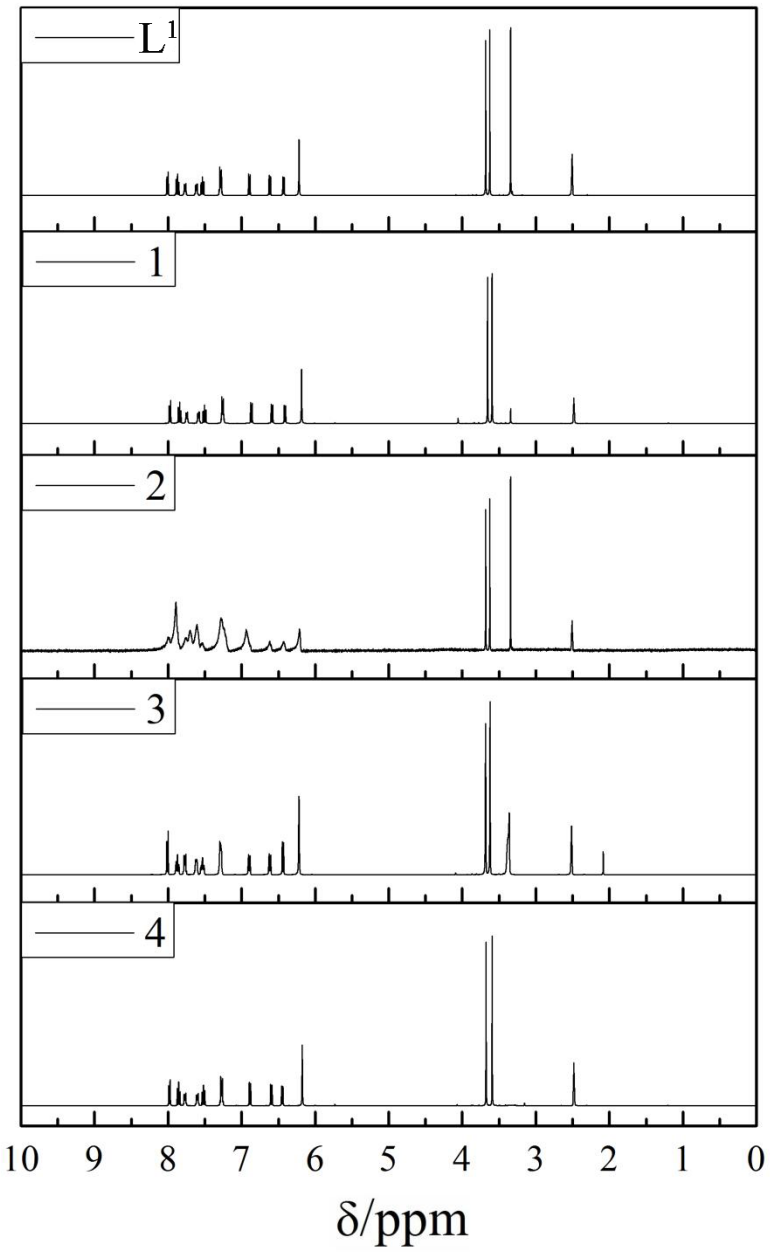

Figure S2. ^{1}H NMR spectra of **L^{1}** and complexes **1**–**4** in DMSO-d_6.

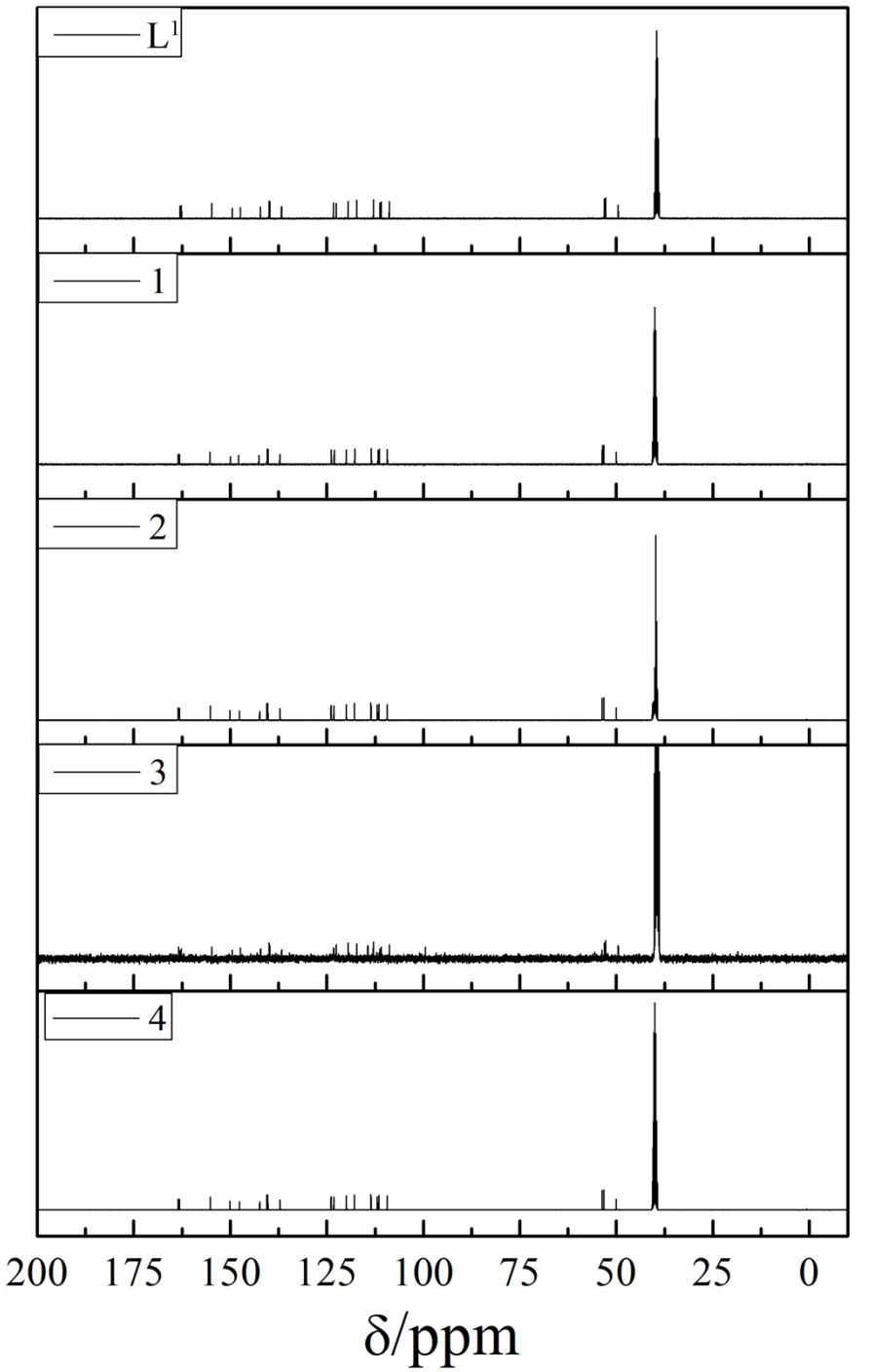

Figure S3. ^{13}C NMR spectra of $\mathbf{L^1}$ and complexes **1**–**4** in DMSO-d_6.

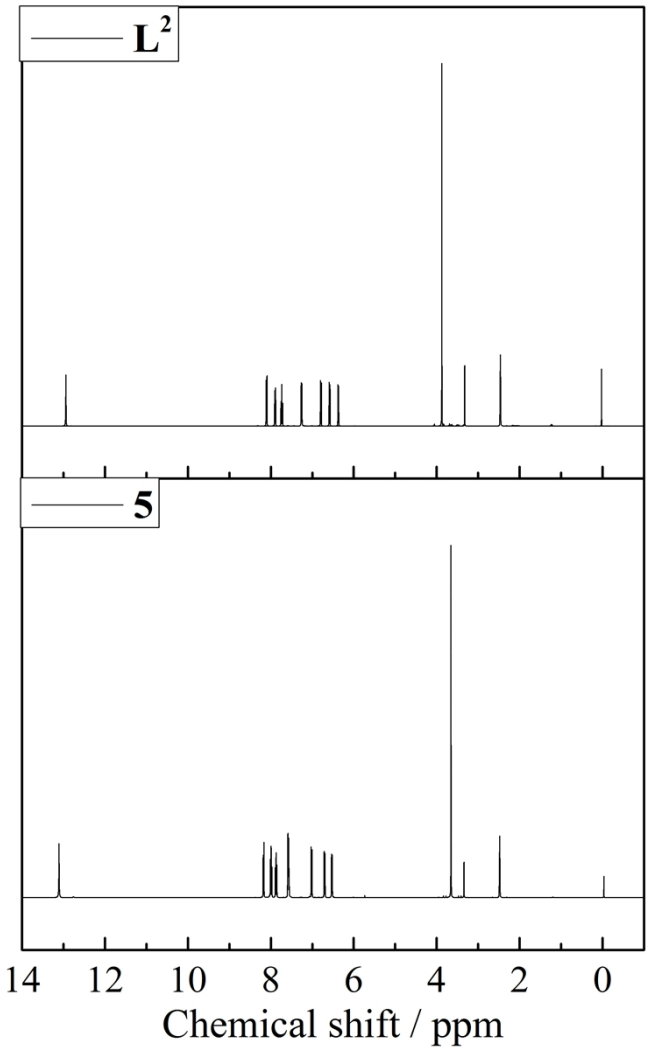

Figure S4. ^{1}H NMR spectra of **L²** and complex **5** in DMSO-d_6.

The ^{1}H NMR spectra of ligand and complexes have been recorded in DMSO-d_6 solution to probe the solution structure. The protons on two pyridine rings (7.2–8.1 ppm) display low-field signals compared that of the protons on benzimidazole group (6.4–7.2 ppm). Further, chemical shift positions of the lower field exist in the pyridyl protons (7.7–8.1 ppm) linking by benzimidazole compared to that pyridyl protons (7.2–7.6 ppm) linking by methylene group (–CH_2–). The single signal of methylene group (–CH_2–) bridging benzimidazole and 6-methoxy-2-pyridinecarboxaldehyde appears at 6.2 ppm. Two intense signals at *ca*. 3.9 and 3.6 ppm are assigned to the –OCH_3 group protons, which possess the same integral area. The lower field signal (3.9 ppm) assigned to the –OCH_3 substituted on the pyridine ring binding to benzimidazole group. For **L²** and **5**, the signal for N*H* proton is also observed at *ca*. 13.0 ppm.

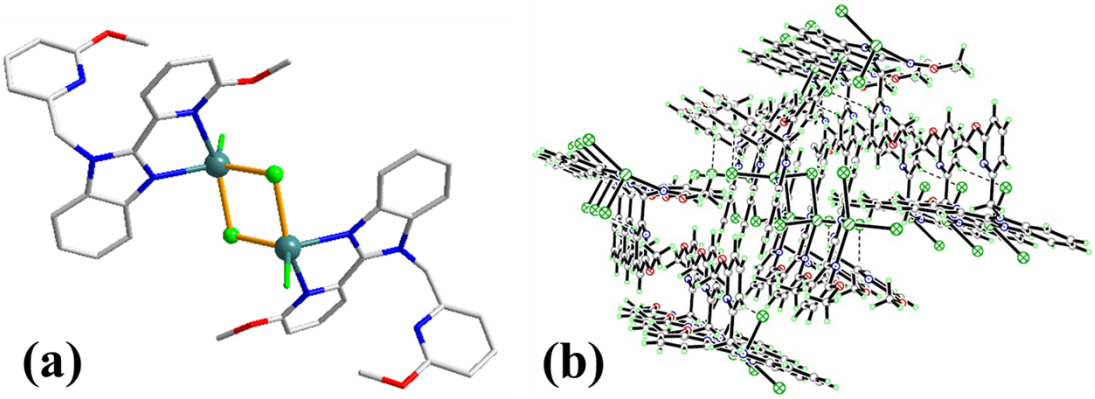

Figure S5. (a) The view of dinuclear structure of complex **2**, the hydrogen atoms are omitted for clarity; (b) Packing diagram of complex **2** generated by hydrogen bonds Cl···H–C along the [100] direction (hydrogen bonds are indicated by dashed lines).

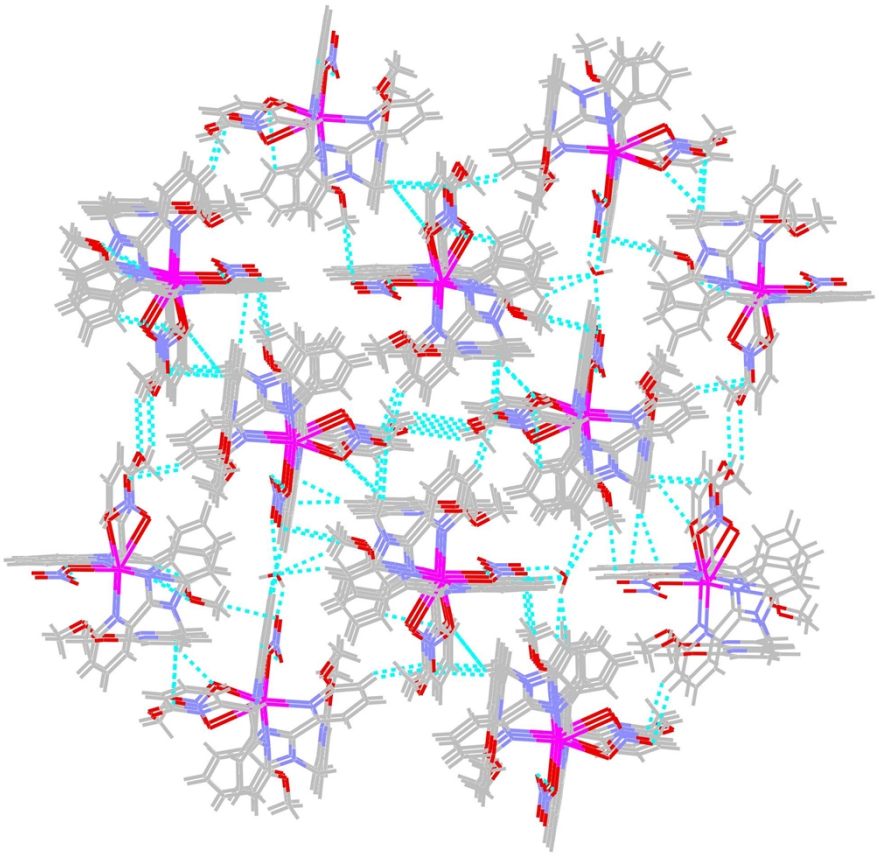

Figure S6. Packing diagram of complex **3** generated by hydrogen bonds O···H–O along the [100] direction (hydrogen bonds are indicated by dashed lines).

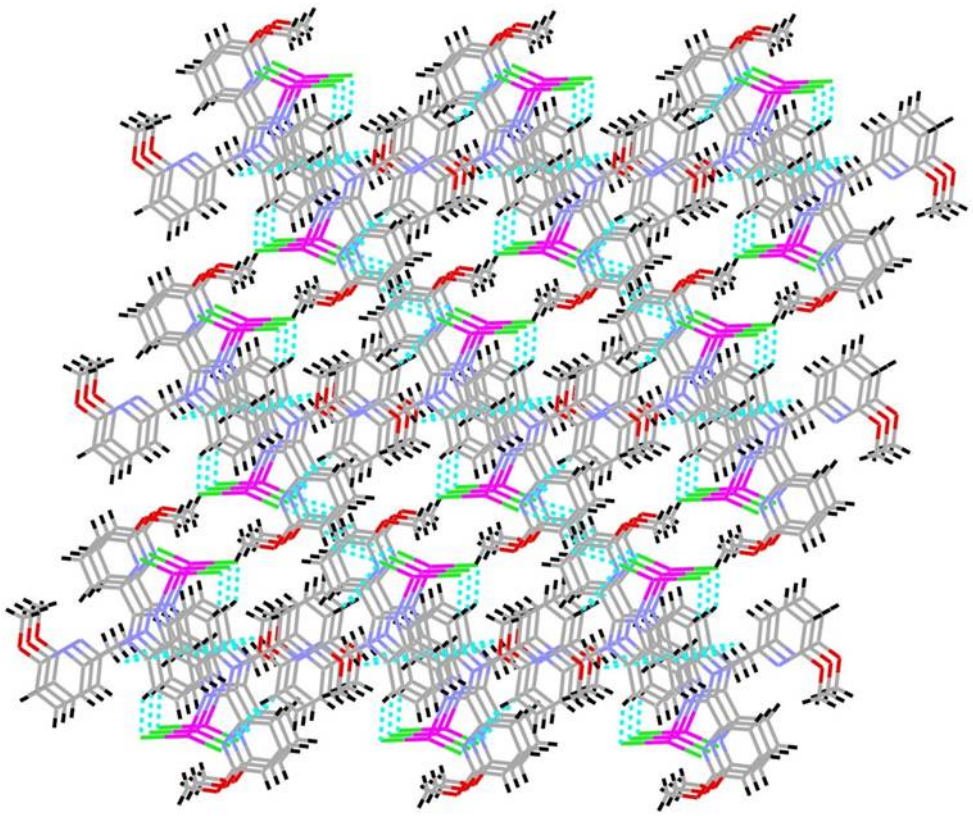

Figure S7. Packing diagram of complex **4** generated by hydrogen bonds Cl···H–O along the [100] direction (hydrogen bonds are indicated by dashed lines).

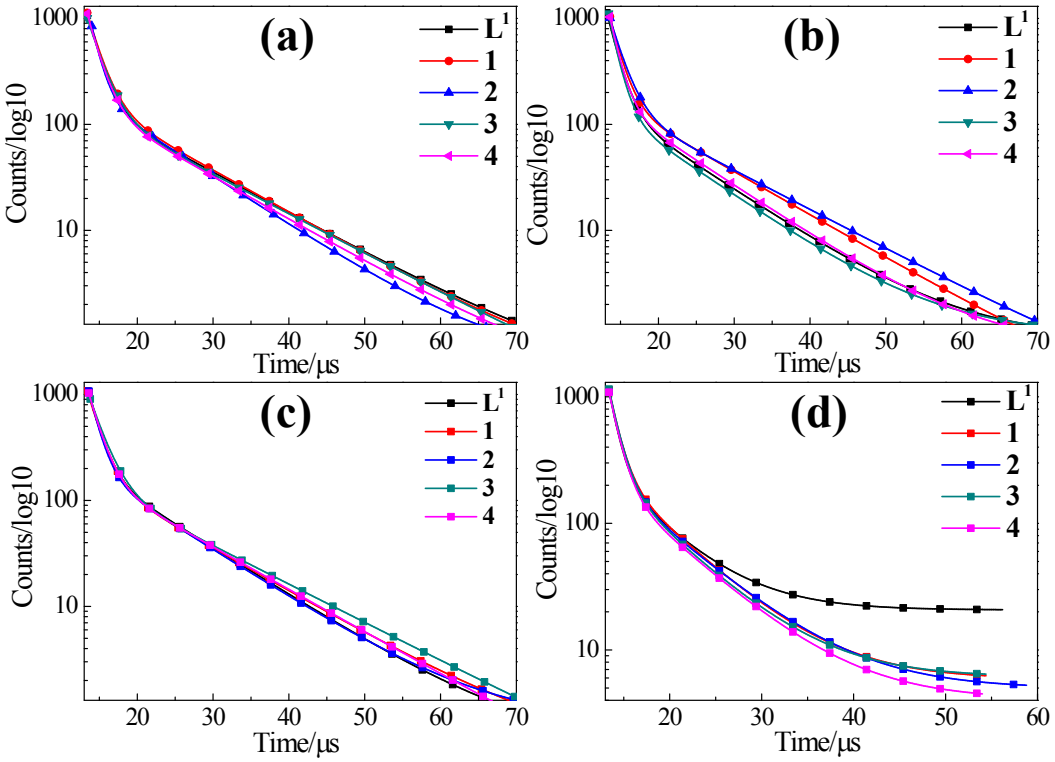

Figure S8. Luminescence decay profiles of **L**^{1} and **1**–**4** monitored at the maximum emission (a: 298 K, CH_3OH; b: 298K, solid state; c: 77K, CH_3OH; d: 77 K, solid state).

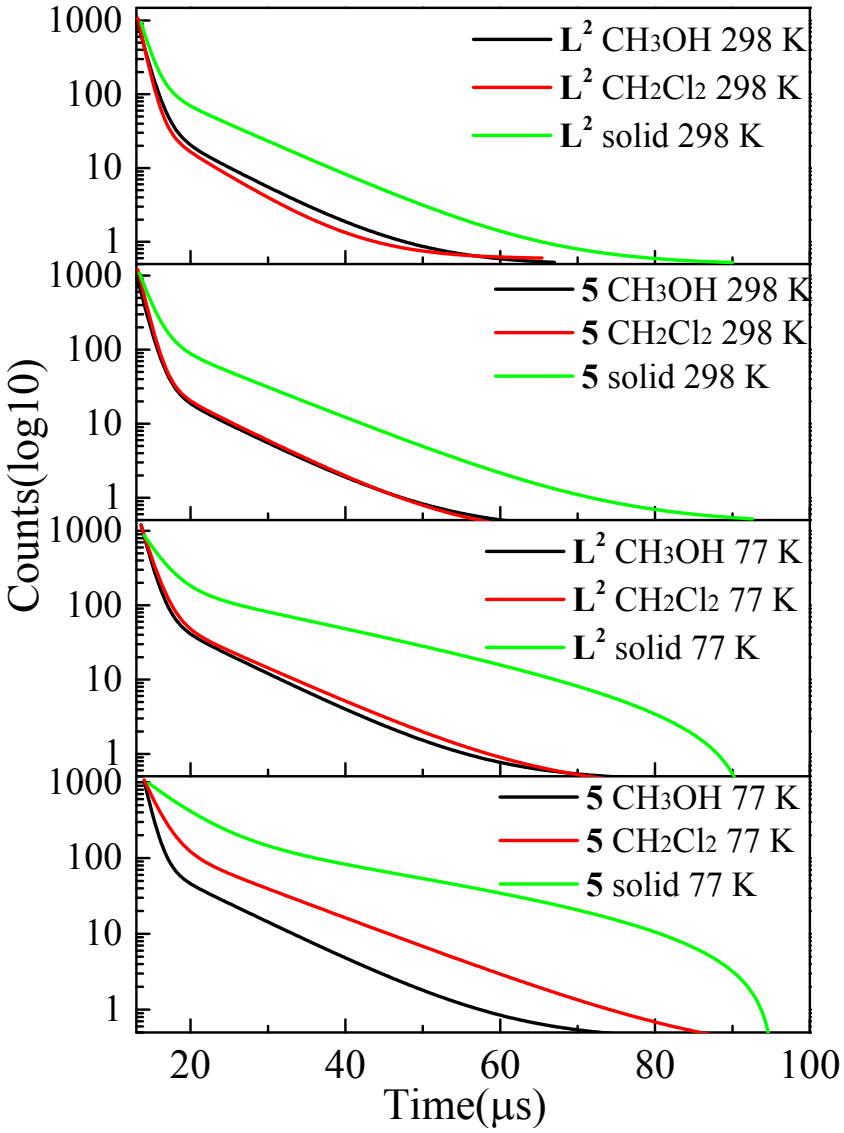

Figure S9. Luminescence decay profiles of **L²** and **5** monitored at the maximum emission.

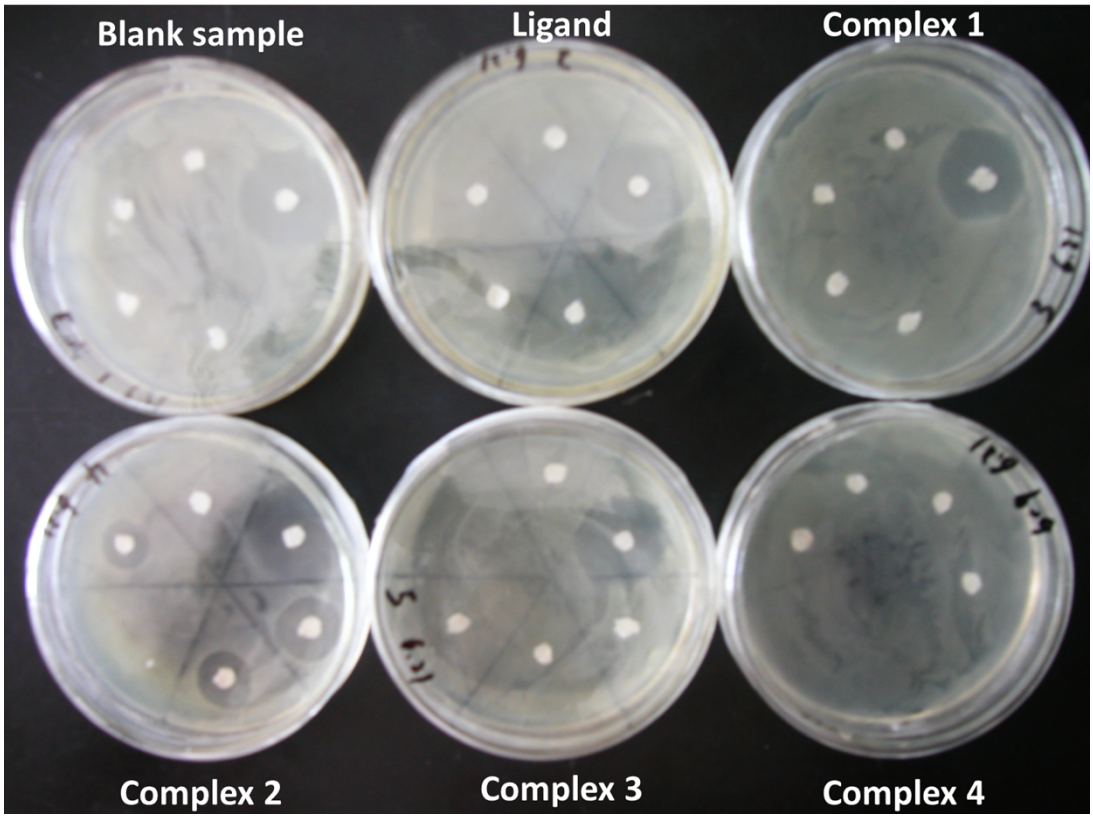

Figure S10. The photo of antibacterial activity for bland sample, ligand $\mathbf{L^1}$ and complexes **1**–**4**.

Antibacterial Activity of $\mathbf{L^1}$ and 1–4

The antibacterial activity of benzimidazole derivatives was carried out with the filter paper method. The solutions of the $\mathbf{L^1}$ and these IIB group metal complexes **1**–**4** were prepared DMSO (dimethyl sulfoxide), and DMSO not containing benzimidazole derivatives was used as a blank control. Stock solutions were diluted with DMSO to 20 mg/mL, 40 mg/mL and 80 mg/mL. The nutrient agar was prepared by dissolving peptone, beef extract, sodium chloride, dextrose, and agar in 1000 mL of distilled water (pH 7.4), and dispended into sterilized petri dishes for inoculation. Suspension of the *Escherichia coli* strain was then plated on the nutrient agar. Sample treated aseptic filter paper was prepared by immersing the paper in the solution of the samples. The plates were divided for five parts as the following treatments: none sample, DMSO, 20mg/mL, 40mg/mL and 80mg/mL of the samples, respectively. The petri dishes were covered, incubated at 35^{o}C for 24 h and then photographed.

The inhibition effects of the samples were demonstrated. Ligand $\mathbf{L^1}$ and their complexes **1**–**4** exhibited varying inhibitory effects toward *E. coli*. The inhibition zones of the $\mathbf{L^1}$ and **1**–**4** were larger than the blank sample, indicating the class of benzimidazole molecules has an inhibitory effect on the growth of the strain. Moreover, the antibacterial activity increased with increasing concentrations of the test solutions. In addition, the inhibition zone of complex **4** is smaller than the others, suggesting that this complex has the best inhibitory activity against *E. coli* compared to other complexes and uncoordinated ligand.